Manufacturing Rev. **12**, 5 (2025)

https://doi.org/10.1051/mfreview/2024026

Manufacturing Review
Available online at:
https://mfr.edp-open.org

Special Issue - Advanced Manufacturing Research – Latest Developments

ORIGINAL ARTICLE OPEN ACCESS

Improving the friction performance of TiAlSiN-coated hard alloy through pulsed magnetic field treatment

Lin Zhang[1], Qiaosong Yan[1], Asha He[2], Zhe Chen[1], Mingxia Wu[1], Yi Yang[1], and Jian Liu[1,*]

[1] School of Mechanical Engineering, Sichuan University, Chengdu, Sichuan 610065, PR China
[2] Department of Industrial Engineering, Sichuan University-Pittsburgh Institute Chengdu, Sichuan 610020, PR China

Received: 31 October 2024 / Accepted: 29 December 2024

Abstract. For processing the difficult-to-cut materials, TiAlSiN coatings have been widely applied to machining tools. Pulse magnetic field treatment, as a novel, fast, and environmentally friendly post-treatment method, can directly modify the finished TiAlSiN-coated tools without causing physical damage. This study investigates the wear resistance of pulse magnetic field-treated TiAlSiN-coated carbide samples under both dry and lubricated friction conditions. Results show that pulse magnetic field-treated TiAlSiN-coated samples exhibit improved wear resistance and friction reduction in both friction environments. In dry friction conditions, the coating's coefficient of friction decreased by 13.73%, resulting in a more stable friction process. In lubricated conditions, the coefficient of friction decreased by 23.46%. Due to the effects of the pulse magnetic field, the hardness of the coating and substrate increased by 6.58% and 3.7%, respectively. The bonding phase Co in the carbide substrate exhibited phase transformation and increased defect density, such as dislocations. These changes enhanced the bonding strength at the coating/substrate interface, thereby improving its mechanical performance and tribological behavior.

Keywords: TiAlSiN coatings / pulse magnetic field / treatment / friction performance

1 Introduction

In the metal processing industry, the utilization rate of coated tools is significantly higher than that of uncoated equipment [1]. TiAlSiN coatings possess excellent comprehensive properties, including higher hardness, thermal stability, and oxidation resistance at high temperatures [2,3], making them suitable for machining hard-to-cut materials. However, during use, the coating eventually begins to peel off due to poor adhesion between the substrate and the coating [4,5]. To address the poor adhesion of silicon-containing hard coatings on hard alloy substrates, researchers [6] proposed a gradient design for TiAlSiN tool coatings using the multi-arc ion plating technique. Additionally, Zhou et al. [7] improved the mechanical and tribological properties of TiAlSiN coatings through annealing treatment. Pulsed magnetic field treatment, as a newly developed green and rapid post-treatment technology, can directly and non-destructively modify TiAlSiN-coated cutting tools and offers more environmentally friendly, contactless, and faster advantages [8,9].

Pulsed magnetic fields have been applied in different processes to improve coating quality [10–12]. Currently, some researchers have applied pulsed magnetic field treatment to coated tools, and results indicate that this treatment can significantly extend the service life of coated tools [13,14]. However, most studies focus on the effects of pulsed magnetic field treatment on the machining performance of processed tools [15–17], with limited research on the friction behavior between hard coatings and workpiece materials under pulsed magnetic field treatment. It is primarily this friction behavior that leads to coating cracking and peeling. To investigate the reasons how the pulsed magnetic field treatment enhances the performance of coated tools, this study applied pulsed magnetic field treatment to TiAlSiN-coated hard alloy samples and evaluated their friction and wear characteristics using a reciprocating friction and wear testing machine.

2 Experimental details

2.1 Coating deposition

The TiAlSiN coating was deposited on mirror-polished hard alloy blocks (WC-12%wtCo) via the multi-arc ion plating method, with sample dimensions of 3084 mm^3. All substrates were ultrasonically cleaned in acetone and ethanol for 20 minutes each. The deposition process utilized eight $Ti_{60}Al_{30}Si_{10}$ alloy targets (atomic percentage, Ø160 mm, purity 99.99%) (see Fig. 1). Before deposition, the chamber temperature was raised to 500 °C, and the

* e-mail: liujian@scu.edu.cn

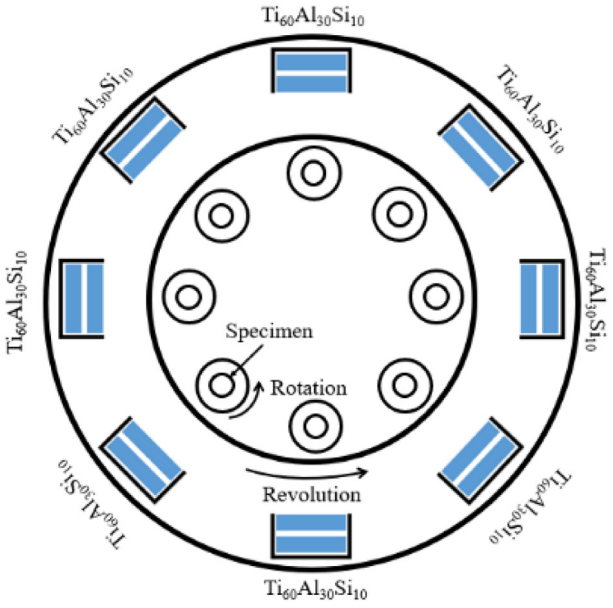

Fig. 1. Schematic diagram of the plasma-enhanced arc ion plating system including the sample fixture and positions of targets.

vacuum level was reduced to 5.0×10^{-3} Pa, with 300 sccm of argon gas introduced. Contaminants and oxide layers on the substrate surface were removed through 30 minutes of argon ion etching at 1000 V bias voltage and 2.0 Pa pressure. The TiAlSiN coating was then deposited for 40 minutes at a cathode current of 140 A on the targets and a DC pulse voltage of 120 V under 3.0 Pa nitrogen gas (purity 99.999%). The deposition temperature and rotation speed were set to 400 °C and 4 rpm, respectively.

2.2 Pulsed magnetic field treatment

The pulsed magnetic field treatment device utilized in this study consists of two main components: a capacitor discharge system and a magnetic induction coil. The periodic discharge of the capacitor system generates a high direct current in the multi-turn magnetic induction coil, thereby applying a high-intensity magnetic field to the specimens under treatment. In this experiment, the WC-12wt%Co hard alloy samples coated with TiAlSiN underwent 20 magnetization treatments in a 1.5T magnetic field, with a pulse interval of 10 seconds, as shown in Figure 2a. Figure 2b displays the magnetic flux density distribution pattern of the samples during the pulsed magnetic field treatment. It is evident that the magnetic flux density on the surface of the hard alloy samples is significantly higher than inside. During the friction process, the surface is the first part to come into contact and undergo wear.

2.3 Tribological test

The tribological performance of TiAlSiN-coated hard alloy samples before and after pulsed magnetic field treatment (PMT) was evaluated on a reciprocating CFT-I friction and wear testing machine using a GCr15 steel ball (6 mm diameter) as the counter material, as shown in Figure 3. The friction environments were categorized into dry friction (Dry) and cutting fluid friction (CF). The cutting fluid was a water-soluble cutting fluid prepared by mixing with distilled water at a 1:15 ratio for CF(Triethanolamine as the main component).

Under the cutting fluid friction condition, the fluid level was maintained 3–4 mm above the sample surface to ensure sufficient lubrication in the contact area. Specific tribological testing parameters are shown in Table 1.

2.4 Characterization

After the tribological tests, the wear morphology and elemental distribution of the TiAlSiN coating and GCr15 steel ball were examined using a Phenom Pro scanning electron microscope (SEM) system equipped with an energy-dispersive spectrometer (EDS). The microhardness HHH of the TiAlSiN coating before and after MT treatment was measured using an Anton Paar G200 Nano indenter. To minimize the influence of the substrate on the film properties, the maximum test load was set to 10 mN, with an indentation depth of 130–140 nm, which is less than 10% of the coating thickness. The Vickers hardness HV3 of the hard alloy substrate was measured with a Wilson VH1150 Vickers hardness tester, using a load of 300 N and a hold time of 15 seconds. The adhesion strength between the coating and substrate was quantitatively analyzed using an MFT-4000 material surface performance tester. The test load was gradually increased from 0 N to 150 N, with a loading rate of 100 N/min and a total scratch length of 5 mm. The residual stress of the coated tool was characterized using X-ray residual stress analysis equipment (X'Pert3, MRD, Malvern Panalytical).

The wear rate W of the GCr15 steel ball was calculated using equation (1), where V (mm^3) is the wear volume, $F(N)$ is the applied load, and L (m) is the total sliding distance.

$$W = \frac{v}{F \times L}. \tag{1}$$

The wear volume of the GCr15 steel ball is calculated by formula (2) and (3) respectively.

$$V = S \times l \tag{2}$$

$$V = \frac{\pi h}{6}(3r^2 + h^2) \tag{3-1}$$

$$h = R - \sqrt{R^2 - r^2} \tag{3-2}$$

In formula (2), l (mm) represents the length of wear markings and S (mm^2) represents the cross-sectional area of coating wear; In formula (3-1) and (3-2), r (mm) represents the dual ball wear spot's radius and h (mm) represents the dual ball wear's height.

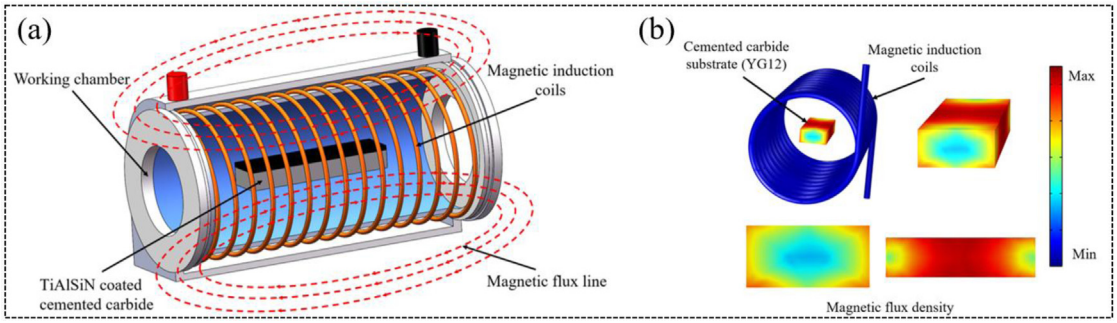

Fig. 2. (a) Schematic diagram of pulsed magnetic field treatment (b) Magnetic flux distribution on the cemented carbide specimen.

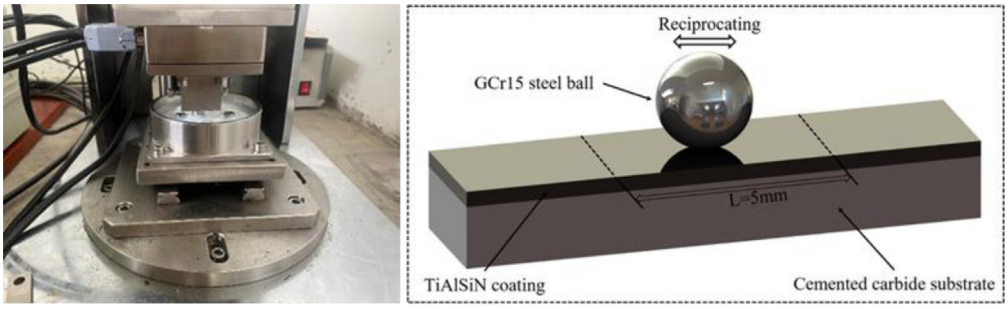

Fig. 3. Schematic diagram of tribological test.

Table 1. Parameters of tribological test.

	Normal load (N)	Reciprocating speed (m/s)	Reciprocating length (mm)	Time (min)
Dry	20	0.1	5	40
CF	80	0.1	5	40

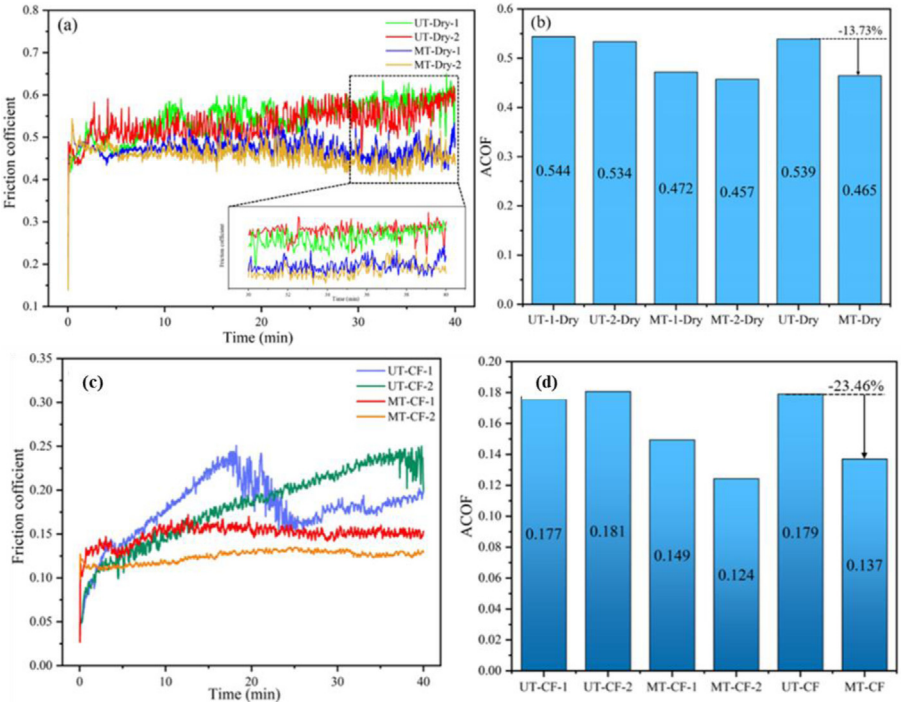

Fig. 4. Coefficient of friction of TiAlSiN coating.

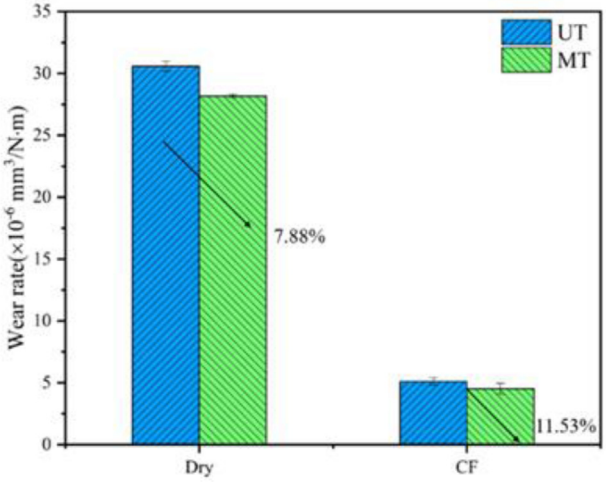

Fig. 5. Wear Rate of GCr15 steel ball.

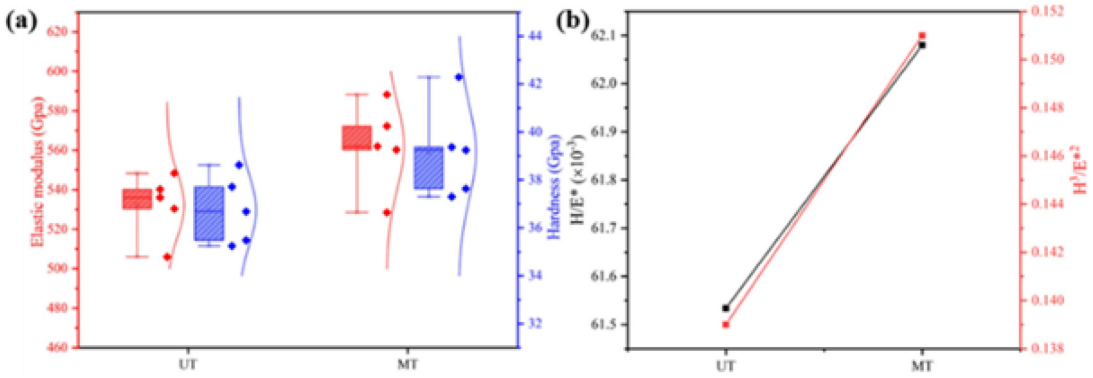

Fig. 6. Indentation hardness, elastic modulus, H/E* and H3/E*2 ratios of the TiAlSiN coating on cemented carbides before and after MT.

3 Results and discussion

3.1 Friction and wear

Figure 4 shows the coefficient of friction variation curves of the pulsed magnetic field-treated sample and the untreated sample under different friction conditions. In both friction conditions, the coefficient of friction decreased after treatment. The average coefficient of friction decreased by 13.73% and 23.46% under dry friction and cutting fluid conditions, respectively. Interestingly, the reduction in coefficient of friction was more significant in the presence of cutting fluid. The wear of the GCr15 counter ball also decreased, with reductions of 7.88% and 11.53% in dry friction and cutting fluid environments, respectively (Fig. 5).

3.2 Mechanical properties of the coating

The hardness and elastic modulus of the coating material are crucial for its wear resistance. After treatment, the hardness and elastic modulus of the TiAlSiN coating increased by 6.58% and 5.64%, respectively (Fig. 6a), which allows the coating to better withstand external pressure, reduce the frictional contact area, and lower the coefficient of friction. In addition, the toughness of the coating improved after treatment, with the ratios of H/E*和 H^3/E^{*2} increasing by 0.89% and 8.63%, respectively (Fig. 6b), indicating an enhanced resistance to plastic deformation.

Figure 7 shows the indentation morphology of the TiAlSiN coating before and after pulsed magnetic field treatment. For the untreated sample (UT), several large and long cracks, along with many short cracks, can be clearly observed around the coating indentation. After pulsed magnetic field treatment, the number of cracks decreased, and the crack lengths were significantly shorter than in the untreated sample. This indicates that the pulsed magnetic field treatment improved the adhesion strength between the TiAlSiN coating and the hard alloy substrate and had an effect in inhibiting crack propagation. To quantitatively analyze the changes in adhesion strength of the TiAlSiN coating before and after pulsed magnetic field treatment, further scratch tests were conducted, and the results are shown in Figure 8.

After pulse magnetic field treatment, the adhesion strength of the coating increased from 50.48 N to 58.19 N, representing a 15.27% improvement. This result aligns with the findings from the Rockwell indentation test, indicating that the adhesion strength of the coating improved following treatment, which also enhanced its

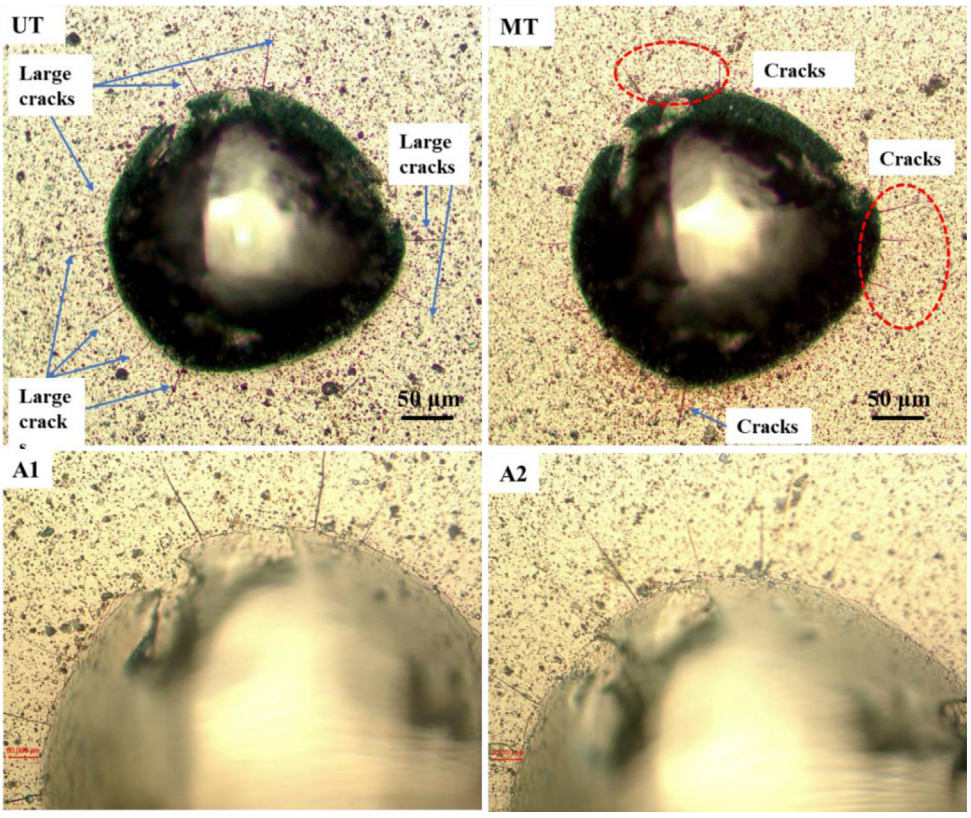

Fig. 7. Indentations made with 60-kg load in TiAlSiN coating.

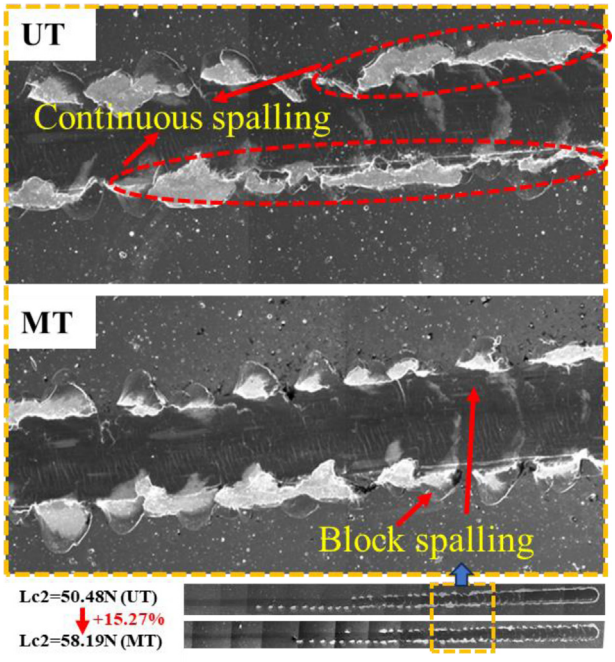

Fig. 8. Coating adhesion before and after pulsed magnetic field treatment.

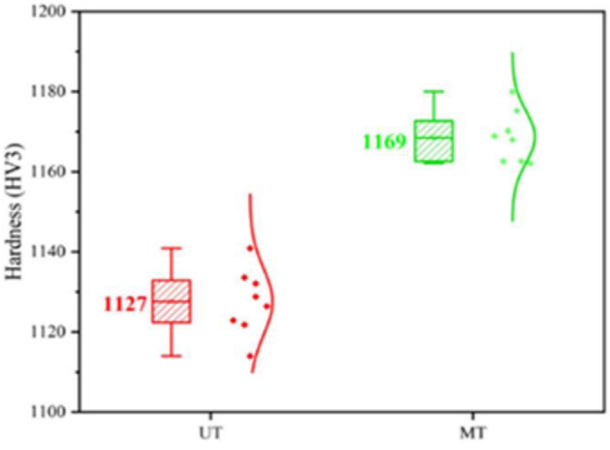

Fig. 9. Changes in the surface Vickers hardness HV3 of the hard alloy samples before and after pulse magnetic field treatment.

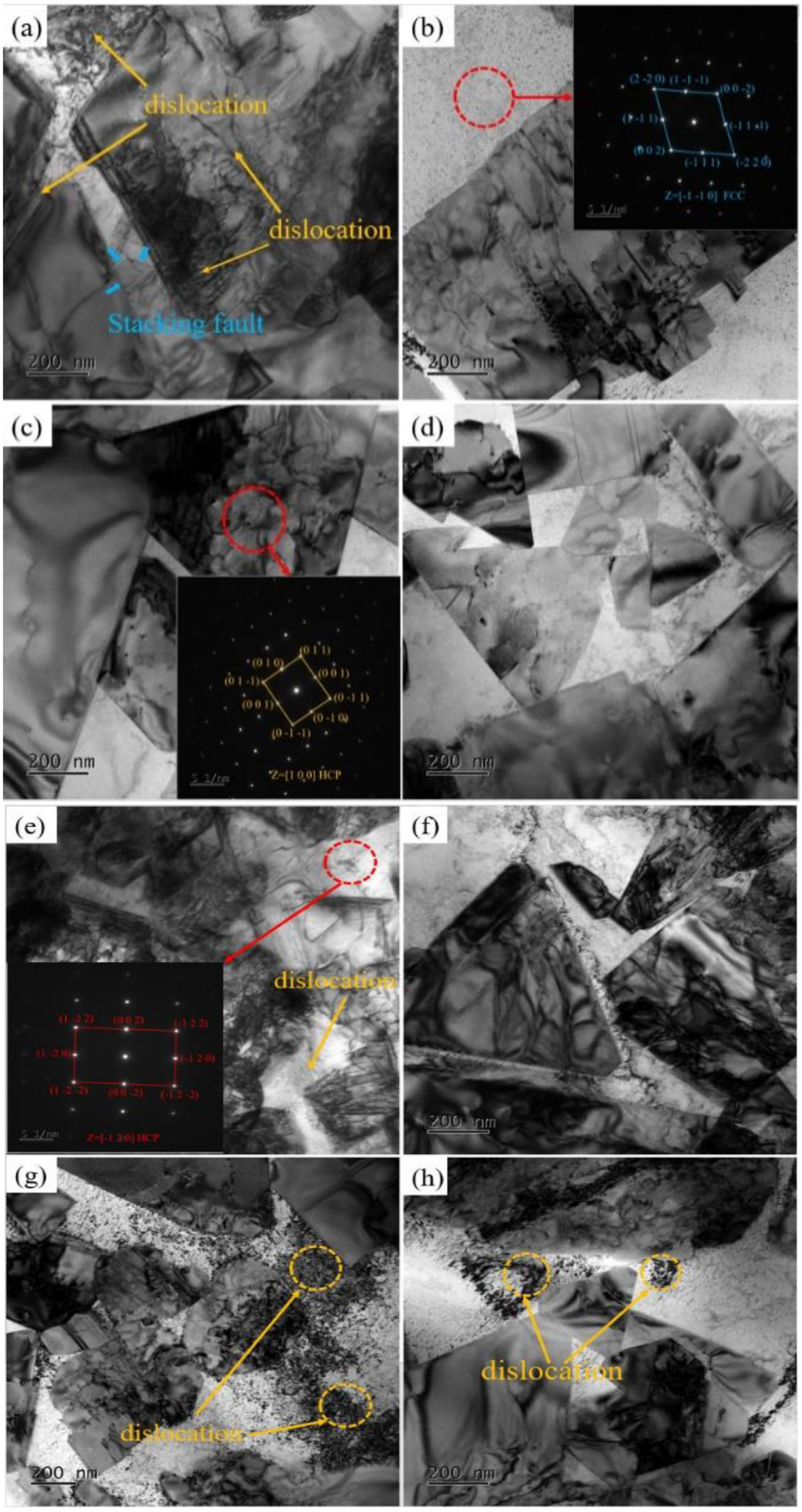

Fig. 10. TEM microstructural morphology of pulsed magnetic field treated and untreated WC-12wt% Co cemented carbide and selected electron diffraction patterns: (a-d) UT; (e-h) MT.

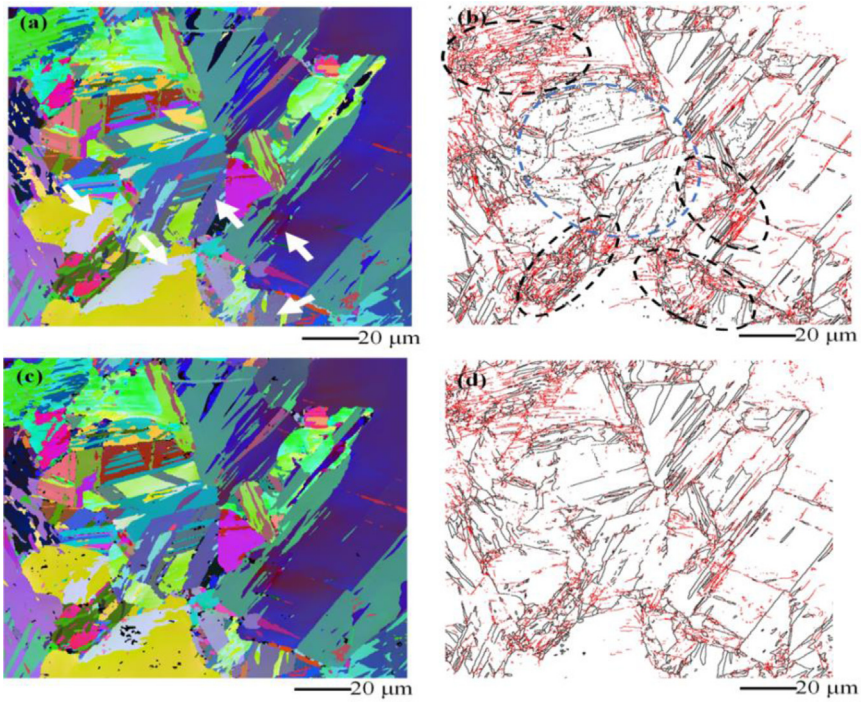

Fig. 11. Comparative in-situ EBSD images of Co before and after pulse magnetic field treatment: (a), (c) Co grain orientation maps; (b), (d) Co grain boundary maps.

wear resistance. From the enlarged local images of the later stages of scratching, it can be observed that untreated samples formed a continuous spallation zone. In contrast, samples treated with the pulse magnetic field did not exhibit continuous spallation, only showing some localized flaking. This is related to the improvement in their crack propagation resistance. Furthermore, Figure 9 shows thechanges in the microhardness of the cemented carbide substrate before and after pulse magnetic field treatment. After the treatment, the microhardness of the substrate increased by 3.73%. The reduction in the hardness difference between the substrateand the coating improves the adhesion of the coating to the substrate.

3.3 Pulsed magnetic field effects on the substrate

The hard alloy substrate provides strong support for the coating, with Co in WC-12%Co being a ferromagnetic material highly sensitive to magnetic fields. The bonding phase changes in the metal-ceramic substrate significantly impact the coating, exhibiting a pronounced substrate effect.

Figure 10 shows the TEM microstructure and diffraction spots of the hard alloy before and after pulse magnetic field treatment. Figures 10a and 10b illustrate the lamellar structure and dislocation morphology of the Co phase in the untreated hard alloy. After pulse magnetic field treatment, the lamellar dislocations almost disappeared (Figs. 10c, 10d), while the dislocation density increased significantly.

Figure 11 shows that, before and after pulse magnetic field treatment, the grain orientation in certain regions of the Co sample changed, as indicated by the arrowed areas, where the change direction aligns with the orientation of adjacent grains. The energy input from the pulse magnetic field caused atoms to shift and migrate from equilibrium states in regions with higher distortion energy, leading to local rearrangements utilizing crystal defects. Figures 11b and 11d show the grain boundary maps before and after pulse magnetic field treatment, with red lines representing low-angle grain boundaries and black lines representing high-angle grain boundaries. In the regions circled in black, the density of low-angle grain boundaries decreased significantly, while the dotted high-angle grain boundaries in the blue-circled region disappeared, resulting in an overall homogenization that reduces grain boundary energy, thereby contributing to greater material stability.

Before magnetic field treatment, the repulsive force between partial dislocations was balanced with the stacking fault energy. The input of external energy caused stacking faults to transform, and the magneto strictive vibration induced by the pulse magnetic field provided the driving force for this transformation, thus triggering phase transformation. After pulse magnetic field treatment, the phase transformation of the Co binding phase on the hard alloy surface and the lattice constant variations of the WC phase influences the lattice mismatch between the substrate and the growing coating [18,19].

4 Conclusions

The application of a pulsed magnetic field increases the wear abrasion performance of TiAlSiN coatings produced on carbide substrates. In dry friction and cutting fluid

friction settings, the average coefficient of friction of TiAlSiN coatings was lowered by 13.98% and 29.83%, respectively. The wear rate of the coating decreased by 21.49% for dry friction, corresponding to the coefficient of friction. Furthermore, because of the reduced adhesive wear, the friction process is more stable. The coating wear width was reduced by 4.6% under cutting fluid friction conditions.

The improvement of TiAlSiN coatings' friction reduction and wear resistance is closely related to the improvement of mechanical characteristics caused by an increase in residual compressive stress within the coating. The increased resistance of the coating to external loads slows the emergence and expansion of cracks and increases the resistance to plastic deformation, which aids in reducing the degree of wear of the coating by the GCr15 steel balls and preventing the hard coating material from participating in the friction behavior as abrasive particles that aggravate the wear. The increase in residual compressive stress within the coating is thought to be the result of the combined effect of the bonded phase's Co-phase phase transition on the surface of the cemented carbide substrate after the pulsed magnetic field treatment, an increase in the density of dislocations and other defects affecting the lattice mismatch between the substrate and the growing coating, and a change in the stress field at the substrate/coating interface.

Pulsed magnetic field (PMF) still faces challenges. Despite its potential to enhance coating performance, ensuring consistency and reliability in large-scale industrial production remains a significant hurdle. Additionally, further research is needed to verify whether PMF technology is equally effective for other types of coating materials or composites.

Funding

The authors wish to acknowledge the financial support by the National Natural Science Foundation of China (No. 51975390 and No. 52205490).

Conflicts of interest

The authors declare that they have no known competing financial interests or personal relationships that could have appeared to influence the work reported in this paper.

Data availability statement

Not applicable.

Author contribution statement

Lin Zhang: Investigation, Methodology, Writing – original draft. QiaosongYan: Methodology, Software. Asha He: Data curation. Zhe Chen: Validation.Yi Yang: Formal analysis. Mingxia Wu: Supervision. Jian Liu:Conceptualization, Funding acquisition, Project administration, Writing–review & editing.

References

1. J. Rech, Influence of cutting tool coatings on the tribological phenomena at the tool-chip interface in orthogonal dry turning, Surf. Coat. Technol. **200** (2006) 5132–5139
2. V.H. Derflinger, A, Schütze, M. Ante, Mechanical and structural properties of various alloyed TiAlN-based hard coatings, Surf. Coat. Technol. **200** (2006) 4693–4700
3. O. Durand-Drouhin, A.E. Santana, A. Karimi, V.H. Derflinger, A. Schütze, Mechanical properties and failure modes of TiAl(Si)N single and multilayer thin films, Surf. Coat. Technol. **163** (2003) 260–266
4. A. Pandey, S. Dutta, R. Prakash, S. Dalal, R. Raman, A.K. Kapoor et al. Growth and evolution of residual stress of AlN films on silicon (100) wafer, Mater. Sci. Semiconduct. Process. **52** (2016) 16–23
5. W. Tillmann, M. Dildrop, Influence of Si content on mechanical and tribological properties of TiAlSiN PVD coatings at elevated temperatures, Surf. Coat. Technol. (2017) 321
6. W. Peng, X.U. Changqing, C. Fei, S.I. Songhua, Z. Shihong, L. Jiagang, Preparation and cutting performance of TiAlSiN gradient coating by multi-arc ion plating, China Surf. Eng. (2019)
7. J. Zhou, X. Fan, H. Chen, D. Feng, Effect of multi-arc current on the microstructure and properties of TiAlSiN coating on zircaloy-4 alloy, J. Mater. Res. Technol. (2023)
8. Q. Shao, G. Wang, H. Wang, Z. Xing, C. Fang, Q. Cao, Improvement in uniformity of alloy steel by pulsed magnetic field treatment, Mater. Sci. Eng. A (2021) 799
9. Y. Zhang, C. Fang, Y. Huang, W. Guo, Z. Xing, H. Wang et al., Enhancement of fatigue performance of 20Cr2Ni4A gear steel treated by pulsed magnetic treatment: influence mechanism of residual stress, J. Magn. Magn. Mater. **540** (2021) 168327
10. Z. Chen, H. Zhou, M. Li, G. Zhang, C. Xu, F. He, Effect of magnetic field waveform on microstructure and properties of laser cladding, Mater. Lett. **X**
11. Y. Hu, L. Wang, J. Yao, H. Xia, R. Liu, Effects of electromagnetic compound field on the escape behavior of pores in molten pool during laser cladding, Surf. Coat. Technol. **383** (2019) 125198
12. Z. Wang, Y. Huang, W. Guo, D. Shan, Z. Xing, H. Wang, Effect of high intensity pulsed magnetic field (30T) on microstructure and tribological properties of Ni-based coatings, Mater. Lett. (2023) 134639
13. H. Fei, H. Wu, X. Yang, J. Xiong, L. Zhang, Z. Chen et al. Pulsed magnetic field treatment of cBN tools for improved cutting performances, J. Manufactur. Process. (2021) 69
14. L. Zhang, Z. Chen, H. Wen, M. Wu, Y. Yang, K. Jiang, et al. Modification effects of the pulsed magnetic field on the coated cemented carbides tool for enhanced mechanical and cutting performances, Int. J. Refract. Metals Hard Mater. (2023)
15. L. Jian, W. Can, Y. Gang, W. Libo, W. Lin, W. Xiuli et al., A novel combined electromagnetic treatment on cemented carbides for improved milling and mechanical performances, Metall. Mater. Trans. A **49** (2018) 1–11
16. Q. Li, Y. Yang, Y. Yang, P. Li, J. Liu, M. Wu, Enhancing the wear performance of WC-6Co tool by pulsed magnetic field in Ti-6Al-4V machining, J. Manufactur Process. (2022)

17. Y. Yang, Y. Yang, Q.Q. Li, Y. Qin, G. Yang, B. Zhou, et al. An eco-friendly pulsed magnetic field treatment on cemented carbide (WC-12Co) for enhanced milling performance, J. Clean. Product. (2022) 340
18. M. Hou, W. Yan, G. Song, G. Wu, Y. Ji, W. Jiang, Z. Wang, W. Qian, C. Cai, Zhipeng. Effects of different distribution of residual stresses in the depth direction on cutting performance of TiAlN coated WC-10wt%Co tools in milling Ti-6Al-4V, Surf. Coat. Technol. (2020) 397
19. G.E. Totten, M. Howes, T. Inoue, Handbook of Residual Stress and Deformation of Steel (ASM International 2002)

Cite this article as: Lin Zhang, Qiaosong Yan, Asha He, Zhe Chen, Mingxia Wu, Yi Yang, Jian Liu, Improving the friction performance of TiAlSiN-coated hard alloy through pulsed magnetic field treatment, Manufacturing Rev. **12**, 5 (2025), https://doi.org/10.1051/mfreview/2024026